Shock wave mechanics in porous ceramic assemblies

P. Boogerd,[a] H. J. Verbeek, M. Stuivinga, and A. C. Van der Steen
TNO Prins Maurits Laboratory, P.O. Box 45, 2280 AA Rijswijk, The Netherlands

J. Schoonman
Laboratory for Applied Inorganic Chemistry, Delft University of Technology, P.O. Box 5045, 2600 GA Delft, The Netherlands

(Received 25 July 1994; accepted for publication 30 January 1995)

The propagation of shock waves in ceramic particle assemblies is described with a simple mechanical model. Shock wave velocities in particle assemblies of BeO, SiC, and UO_2 are predicted within 9% from measurements at a different density, and solid material properties. Assembly properties of several BeO, SiC, and UO_2 porous assemblies are compared. The results indicate that it is possible to discriminate between material effects and assembly effects. This yields the possibility of calculating shock waves in a porous ceramic assembly using generally applicable assembly properties, and the solid material properties of the ceramic. © *1995 American Institute of Physics.*

I. INTRODUCTION

When shock waves are applied to porous assemblies, e.g., for the compaction of ceramic powders, the effect of the shock wave on the structure of the material is very important. Several theoretical models for the propagation of a shock wave in a porous assembly[1–3] were developed based on a continuum description of the porous assembly. These models, however, only consider overall assembly parameters, such as the density.

So far only micromechanical simulations have shown promising results in describing shock waves in particle assemblies while including their effect on the particle structure.[4,5] These simulations, however, require a large computational capacity to simulate even the smallest assemblies.

The present model is a description of a shock wave traveling through a collection of solid spheres. The model assumes that inside these spheres the shock wave travels as if through a solid, but that a delay is caused during the transmission of the shock from sphere to sphere. This delay occurs due to the deformation of the spheres, when the shock wave is transmitted.

The model aims to predict the shock wave velocities in porous assemblies using data available for assemblies of the same material at other densities, while in the meantime acquiring a description of the changes in a particle assembly due to the passage of a shock wave.

The model describes shock wave equilibrium conditions, and incorporates no absorption of shock energy. No energy dissipation effects due to, e.g., surface melting, friction, and such are included. The model describes a shock wave traveling through a porous assembly. Only the longitudinal velocity component normal to the shock wave plane and the corresponding stresses are considered. The solid spheres are assumed to behave as a solid material under equilibrium shock wave conditions. The model is valid only for assemblies in which compaction mainly occurs due to particle deformation and does not incorporate particle fracture.

First the principles of the model are introduced. It is shown that the concept of shock wave delay due to particle deformation is supported by experimental evidence, and the approximations necessary for the model are discussed. These lead to an expression for the stress in the solid spheres.

Second the model itself is developed in two steps, i.e.,

(a) the determination of the particle deformation in a loosely packed assembly in which the spheres have only point contacts, and
(b) the formulation of the relation between the deformation in a loosely packed, and a precompacted assembly.

Third the deformation curves of three ceramics at several densities are calculated, and discussed.

Fourth the relation between the deformation curves in two precompacted assemblies with different densities is formulated.

And finally, these relations are applied to predict the shock wave velocity in a porous assembly, from experimental data obtained at another density.

II. THEORY

The model is based on the assumption that a certain contact area is created during the transmission of a shock wave from particle to particle. This contact area is created by deformation of the particles.

Several experimental observations clearly suggest this deformation effect: i.e.,

(a) The shock wave velocity in a porous assembly is always less than in a fully dense sample of the same material at the same stress level;[6]
(b) the density of a porous assembly is changed irreversibly by the passage of a shock wave;
(c) after passage of a shock wave through a porous assembly the compact shows micromechanical effects. Severe plastic deformation is observed at the grain

[a]Also with: Laboratory for Applied Inorganic Chemistry, Delft University of Technology, P.O. Box 5045, 2600 GA Delft, The Netherlands.

boundaries in metals[4,5] and ceramics.[7,8] Local melting and decomposition also occur specifically at grain boundaries, and not inside the grains.

Simulations of shock waves through an array of metal cylinders by Flinn *et al.*[4] and Gao and co-workers[5] show a good correlation with the experiments. In these simulations the particles show deformation in and immediately after the shock wave front. This also indicates that the particle-particle contact surface area has to increase in order to allow the transmission of the stationary shock stress.

The stationary shock stress in a porous assembly is the constant stress attained a short distance after the front of a shock wave. For shock waves in porous substances in particular the shock wave has a blurred precursor due to shock reflections at the particle surfaces.[9]

The present model only applies to the situation in which the relative density is large enough to guarantee particle contact. Initial particle contact can be assumed to exist above the loose packing density.[10] The density of a random loose packing of randomly shaped particles varies between 45% theoretical maximum density (TMD) and 55% TMD.[10] At lower density the effect of particle rearrangement is too profound. This effect will also delay the shock wave, but is not considered in the model.

The model also does not incorporate particle fracture at stresses well above those at which plastic deformation occurs. It only describes the plastic-flow regime and should not be applied to other regimes.

In the model the behavior of a porous assembly is described with an array of solid spheres. In the solid spheres the shock stress is assumed to remain constant. Furthermore it is assumed that the shock stress components perpendicular to the shock wave direction compensate each other. In reality the particles in a porous ceramic assembly will hardly ever be spherical; however, a large number of randomly shaped particles with random orientation can be described with an array of spheres as a good first approximation.

Furthermore, for the current model it is assumed that the many small shock waves inside the particles can be described with one collective planar shock wave. In addition, it is assumed that this averaged shock wave can be described with shock wave parameters that apply to bulk solid materials.

For the deformation model it is necessary to know the average stress in the solid material in the porous assembly. By using an analogy with a static situation this stress inside the solid material can be approximated. The average stress in the solid material can then be calculated from the assembly density and the stress on the assembly.

In the experiments, used to determine shock wave velocities in porous assemblies, a planar shock wave, of stress σ_{assembly} is introduced in the porous assembly by planar impact.[6]

In a static situation the average internal stress in the solid material $\sigma_{\text{solid,static}}$, can be calculated from the solid part of the cross-sectional surface of the assembly. In a cross section of a porous assembly, with a relative density ϵ compared to the solid, the solid surface covers a surface of ϵ times the total cross section. Thus, the stress $\sigma_{\text{solid,static}}$ in the solid can be found from the stress $\sigma_{\text{assembly,static}}$, on the porous assembly,

$$\sigma_{\text{solid,static}} = \sigma_{\text{assembly,static}} \frac{S_{\text{assembly}}}{S_{\text{solid}}} = \frac{\sigma_{\text{assembly,static}}}{\epsilon}, \tag{1}$$

in which S_{assembly} is the cross-section surface area of the porous assembly and S_{solid} the cross-section surface area of the solid.

An analogous equation can be applied to a dynamic situation if $\sigma_{\text{solid,static}}$ is replaced with the average shock stress σ in the solid phase of the assembly in the plane of shock and $\sigma_{\text{assembly,static}}$ is replaced with the dynamic stress σ_{assembly} on the assembly.

In the present model the shock wave velocity $U_{s,\text{solid}}$ and mass displacement velocity $u_{p,\text{solid}}$ in the solid part of the assembly is calculated with the stress σ calculated with Eq. (1). It should be borne in mind that the $U_{s,\text{solid}}(\sigma)$ and $u_{p,\text{solid}}(\sigma)$ relations that will be used, are basically only valid for solid bulk materials, while the variables used in our derivation have values averaged over the particles. The correct relations between the average variables might differ considerably and even systematically from the relations for the bulk materials. The latter relations are nevertheless used as a first approximation.

Before the stationary shock stress is reached small shock waves of lower stress are already present in the particles. The effect of the solid material densification, due to these waves, on the shape of the particles is not incorporated in the model.

III. MODEL

A. Introduction

The aim of the model is to be able to use shock wave velocity data from a porous assembly to predict shock wave velocities in porous assemblies of the same or perhaps another material at other densities. In addition it aims to describe the microstructural changes in a particle assembly due to the passage of a shock wave.

To develop the model, first the particle deformation in a loosely packed assembly is determined. In a loosely packed assembly there are only point contacts between the spheres, as shown in Fig. 1(a). Any deformation of the spheres is solely due to the shock wave, as shown in Fig. 1(b).

In the second part the relation between the shock wave deformation in a loosely packed assembly and a precompacted assembly are derived. In an assembly precompacted by, for instance, sintering or static pressing the particles are already deformed, before the shock wave arrives, as shown in Fig. 1(c). The shock wave then compresses the particles as shown in Fig. 1(d), which is comparable to the state shown in Fig. 1(b).

In the third part the relation between the shock wave deformation in two precompacted assemblies with a different starting density is derived.

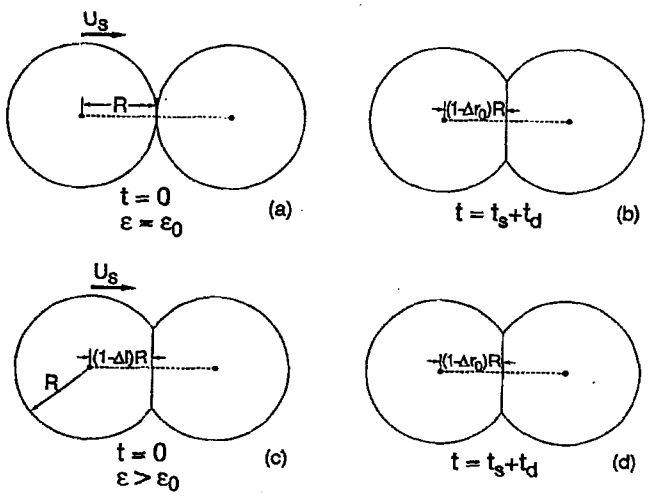

FIG. 1. Schematic representation of impacting spheres: (a) For spheres with a point contact (loosely packed assembly, with a density $\epsilon=\epsilon_0$) at the time the shock wave arrives (with shock wave velocity U_s) at the center of the impacting sphere ($t=0$); (b) for spheres that initially have point contact at the time the shock wave arrives at the center of the target sphere ($t=t_s+t_d$); (c) for spheres with an initial contact surface (precompacted assembly, with a density $\epsilon>\epsilon_0$) at the time the shock wave arrives at the center of the impacting sphere ($t=0$); (d) for spheres that initially have a contact surface at the time the shock wave arrives at the center of the target sphere ($t=t_s+t_d$).

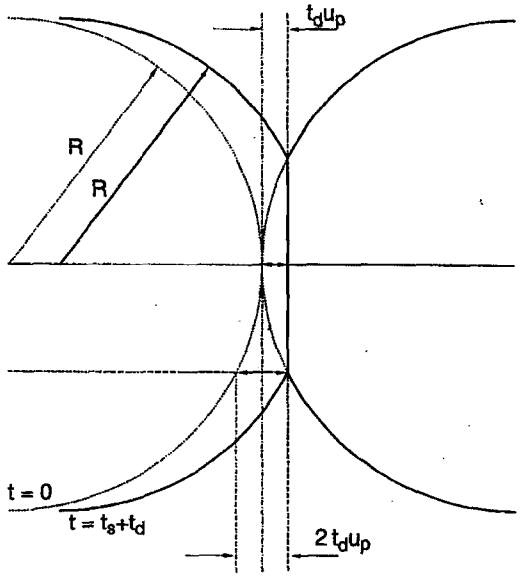

FIG. 2. Schematic representation of impacting spheres with the deformation as a function of the mass displacement velocity u_p. The spheres have only point contact at $t=0$.

In the fourth part this relation is used to calculate the shock wave velocity in a precompacted assembly using the deformation data of a precompacted assembly with an other density.

B. Deformation in a loosely packed assembly

The deformation in the assembly is the result of the transmission and reflection of many small shock waves that travel in different directions and interfere. In the present model this complex situation is treated by the introduction of a delay time t_d. In this delay time the deformation of the spheres is assumed to occur with the mass displacement velocity.

In Fig. 2 the particle is shown when the shock wave arrives at the center of the impacting sphere ($t=0$) and after the transmission of the shock wave, when the particles are fully deformed ($t=t_s+t_d$).

The shock wave velocity through the porous assembly $U_{s,\text{assembly}}$ can be found from the distance traveled and the corresponding time needed. In traveling from particle center to particle center the distance traveled is

$$\Delta x=2R, \tag{2}$$

in which R is the particle radius.

The corresponding time t consists of two parts, i.e., first the time t_s, for the shock wave to travel through the solid material,

$$t_s=\frac{2R}{U_{s,\text{solid}}}, \tag{3}$$

in which $U_{s,\text{solid}}$ is the average shock wave velocity in the solid particles comprising the porous assembly. The second part is the delay time t_d introduced to take into account that the deformation process during the shock wave transmission delays the shock wave.

Introduction of t_d results in the following equation for the shock wave velocity in the porous assembly $U_{s,\text{assembly}}$:

$$U_{s,\text{assembly}}=\frac{2R}{(2R/U_{s,\text{solid}})+t_d}. \tag{4}$$

It is assumed that the delay time t_d is determined by the velocity at which the impacting sphere is deformed. In a vacuum or a medium with a low density such as air the velocity at which the surface of the impacting sphere moves is twice the mass displacement velocity, $2u_{p,\text{solid}}$. The distance over which the surface of the impacting sphere at the edge of the contact surface has travelled at $t=t_d$ is $2t_du_{p,\text{solid}}$ as can be seen in Fig. 2. At the contact surface the material moves with the mass displacement velocity, and this causes the deformation shown in Fig. 2.

We now define a dimensionless deformation parameter Δr_0 as

$$\Delta r_0\equiv\frac{t_du_{p,\text{solid}}}{R}, \tag{5}$$

in which $u_{p,\text{solid}}$ is the average mass displacement velocity of the material in the particle and R is the particle radius. This means that Δr_0 is the relative compression of the sphere due to the shock wave.

Combining Eqs. (4) and (5) gives

$$\frac{1}{U_{s,\text{assembly}}}=\frac{1}{U_{s,\text{solid}}}+\frac{\Delta r_0}{2u_{p,\text{solid}}}, \tag{6}$$

in which $U_{s,\text{assembly}}$ is a function of σ_{assembly}, the shock stress in the porous assembly, and $u_{p,\text{solid}}$ and $U_{s,\text{solid}}$ are functions of σ, the shock stress in the solid phase in the assembly. These two stresses are related through Eq. (1), which makes it possible to determine the $\Delta r_0(\sigma)$ curve as a function of one stress parameter only.

C. Deformation in a precompacted assembly

In an assembly that is precompacted by sintering or static pressing, the particles are already deformed, before the shock wave arrives. If the deformation by pressing or sintering is assumed to be isotropic this initial deformation can be calculated from the initial density. This calculation shown in the Appendix leads to the following expression for the initial deformation Δl:

$$\Delta l = 1 - \left(\frac{\epsilon_0}{\epsilon}\right)^{1/3}, \tag{7}$$

in which ϵ_0 and ϵ are the relative densities of a loosely packed and precompacted assembly, respectively, compared to solid material.

The density of a random loose packing of irregular particles varies between[10] 45% TMD and 55% TMD. In the following Δl is calculated with ϵ_0=50% TMD. The maximum error of about 10% in the relative density leads to a maximum error of about 3% in the initial deformation Δl.

If an assembly is precompacted before a shock wave is applied the particles deform. This initial deformation in the direction of the shock wave is Δl as shown in Fig. 1(c) ($t=0$). It is assumed that the shape of the contact area due to initial deformation is the same as would occur in a shock wave, $\Delta r_0=\Delta l$ [Fig. 1(b), $t=t_s+t_d$]. The deformation of a prepressed or sintered porous assembly can then be related to the curve of a loosely packed assembly.

The shock wave delay in a prepressed or sintered assembly can be calculated analogous to the delay in a loosely packed assembly.

In a precompacted assembly the distance from particle centre to particle center is

$$\Delta x = 2R(1-\Delta l). \tag{8}$$

The time needed for the shock wave to travel through the solid material becomes

$$t_s = \frac{2R(1-\Delta l)}{U_{s,\text{solid}}}. \tag{9}$$

The shock wave velocity in the porous assembly $U_{s,\text{assembly}}$ is then found from

$$U_{s,\text{assembly}} = \frac{2R(1-\Delta l)}{[2R(1-\Delta l)/U_{s,\text{solid}}]+t_d}. \tag{10}$$

The delay time t_d, can now be found from the total deformation, which is the shock wave deformation for the loosely packed assembly Δr_0, minus the initial deformation Δl,

$$t_d = \frac{R(\Delta r_0 - \Delta l)}{u_{p,\text{solid}}}. \tag{11}$$

TABLE I. (a) Parameters of the least-squares, second-order polynomial fit of the shock velocity $U_{s,\text{assembly}}$, in the assembly, to the stress σ_{assembly} for BeO, SiC, and UO_2 at several relative densities ϵ ($U_{s,\text{assembly}} = a_0 + a_1\sigma_{\text{assembly}} + a_2\sigma^2_{\text{assembly}}$). Data are from Marsh (Ref. 6). (b) Parameters of the least-squares second-order polynomial fit of the mass displacement velocity $u_{p,\text{assembly}}$ to the stress σ_{assembly} for BeO, SiC, and UO_2 at several relative densities ϵ ($u_{p,\text{assembly}} = b_0 + b_1\sigma_{\text{assembly}} + b_2\sigma^2_{\text{assembly}}$). Data are from Marsh (Ref. 6).

(a)

Compound	ϵ (% TMD)	a_0 (km s^{-1})	a_1 (km s^{-1} GPa^{-1})	a_2 (km s^{-1} GPa^{-2})
BeO	99.3	$+1.070\times10^{-1}$	-2.413×10^{-2}	$+3.771\times10^{-4}$
	92.4	+8.077	$+2.016\times10^{-3}$	$+3.571\times10^{-4}$
	81.4	+4.019	$+1.085\times10^{-1}$	-4.500×10^{-4}
SiC	97.0	$+1.120\times10^{-1}$	-5.731×10^{-2}	$+5.611\times10^{-4}$
	94.2	+8.772	-1.113×10^{-2}	$+3.158\times10^{-4}$
	72.5	+2.717	$+1.322\times10^{-1}$	-6.898×10^{-4}
UO_2	94.0	+3.802	$+1.378\times10^{-2}$	$+1.013\times10^{-5}$
	57.9	+1.415	$+5.822\times10^{-2}$	-1.810×10^{-4}

(b)

Compound	ϵ (% TMD)	b_0 (km s^{-1})	b_1 (km s^{-1} GPa^{-1})	b_2 (km s^{-1} GPa^{-2})
BeO	99.3	-6.959×10^{-2}	$+3.824\times10^{-2}$	-9.596×10^{-5}
	92.4	$+2.558\times10^{-2}$	$+4.626\times10^{-2}$	-1.589×10^{-4}
	81.4	$+7.877\times10^{-1}$	$+3.460\times10^{-2}$	-3.379×10^{-5}
SiC	97.0	-1.668×10^{-1}	$+4.151\times10^{-2}$	-1.049×10^{-4}
	94.2	-2.848×10^{-1}	$+5.172\times10^{-2}$	-1.857×10^{-4}
	72.5	$+8.844\times10^{-1}$	$+4.328\times10^{-2}$	-8.651×10^{-5}
UO_2	94.0	$+5.662\times10^{-2}$	$+2.244\times10^{-2}$	-4.651×10^{-5}
	57.9	$+6.579\times10^{-1}$	$+3.067\times10^{-2}$	-7.802×10^{-5}

Combining Eqs. (10) and (11) gives an equation analogous to Eq. (6),

$$\frac{1}{U_{s,\text{assembly}}} = \frac{1}{U_{s,\text{solid}}} + \frac{(\Delta r_0 - \Delta l)}{(1-\Delta l)}\frac{1}{2u_{p,\text{solid}}}, \tag{12}$$

in which $U_{s,\text{assembly}}$ is a function of σ_{assembly} the stress on the porous assembly, and $u_{p,\text{solid}}$ and $U_{s,\text{solid}}$ are functions of σ, the stress in the solid phase in the assembly. These two stresses are related through Eq. (1), which makes it possible to determine the $\Delta r_0(\sigma)$ curve as a function of one stress parameter only.

The shock wave deformation of the spheres Δr, which is reached when the stable shock stress is attained, can be calculated from the total deformation Δr_0 and the initial deformation Δl using Eq. (12) and

$$\Delta r = \Delta r_0 - \Delta l. \tag{13}$$

When the Δr_0 curve is known for a certain ceramic the shock wave velocity $U_{s,\text{assembly}}$ in any porous assembly can be calculated with Eq. (12). Because the aim of the present model was not only to find the shock wave velocity, but also to study the effects of the shock wave on the porous assembly, we first analyze the deformation curves before applying them to the calculation of shock wave velocities.

IV. SHOCK WAVE DEFORMATION CURVES

A. Calculations

For the calculation of the particle deformation with Eq. (12), it is necessary to have equations describing the shock wave velocities $U_{s,\text{solid}}$ and $U_{s,\text{assembly}}$ and the mass displacement velocity $u_{p,\text{solid}}$, as a function of the dynamic stress. In this case data were used from Marsh.[6] The shock wave velocity and the mass displacement velocity were correlated to the dynamic stress applied to the assembly σ_{assembly} by a second-order polynomial.

The fits are performed for solid BeO, solid SiC, and solid UO_2 and a number of particle assemblies of these materials. These materials were the only ceramics for which enough data were available. The parameters of the polynomials are shown in Tables I(a) and (b). For the materials data were only available for a limited stress range. The stress ranges within which the data were available are shown in Table II.

Because data for the pure 100% TMD ceramics were not available we used the data of 99.3% TMD BeO, 97.0% TMD SiC, and 94.0% TMD UO_2 to determine $U_{s,\text{solid}}(\sigma)$ and $u_{p,\text{solid}}(\sigma)$.

The values of Δl were calculated with Eq. (7) with ϵ_0=50% TMD. In Fig. 3 all the Δr curves for the ceramics are shown together, plotted against σ, the shock stress in the solid phase in the assembly.

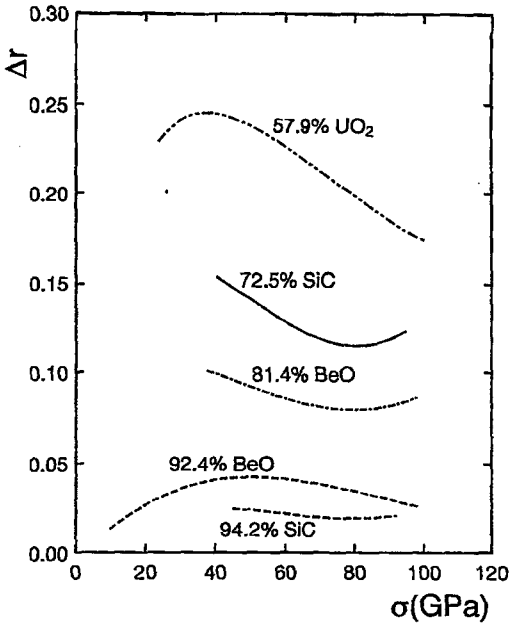

FIG. 3. The shock deformation curves for 81.4% TMD and 92.5% TMD BeO, 72.5% TMD and 94.2% TMD SiC, and 57.9% TMD UO_2. The curves were calculated using data from Marsh (see Ref. 6).

B. Discussion

The deformation curves increase with decreasing relative density ϵ as can be seen in Fig. 3. This can be explained from the fact that in these assemblies (with ϵ>50% TMD) the particles already have an initial contact surface which increases with the density. Therefore, less deformation occurs in the shock wave for an assembly with a high starting density. This leads to a comparatively low Δr curve for assemblies with a high initial density as can be seen in Fig. 3.

In Fig. 3 it can be seen that for BeO, SiC, and UO_2 the deformation shows an overall increase with decreasing relative density. This effect appears to be material independent for these materials. This indicates that the particle deformation depends more on assembly properties than on solid material properties. The results suggest that the deformation curves for the three ceramics are mutually exchangeable.

In Fig. 3 the deformation curves of 57.9% TMD UO_2 and 92.4% TMD BeO show a maximum. The initial rise in the deformation curves can easily be explained. At low stresses the shock wave can be transmitted through a small contact area, so there is little delay.

The deformation curves show a decline for stresses above ~40 GPa. The effect is strongest for low densities. This is an unexpected effect, because the deformation is expected to increase with increasing stress to a theoretical maximum. A possible explanation for this might be the occurrence of particle rearrangement, which was not accounted for in the model.

Because the shock wave compaction that occurs in shocked porous assemblies is a complicated process, involving more than only plastic deformation, the interpretation of the shape of the deformation curves must be approached with care. Furthermore, the simplifications and assumptions that have been applied in the model might affect this shape. Due to the lack of sufficient data on the compaction process in relation to the shock state, thorough study is, as yet, not possible.

However, when the deformation curves are used as an intermediate to calculate the Hugoniot of a porous material only the relative magnitude of the two different deformation curves is important. Calculations show that an error of 10% in the value of the deformation would result in an error of only about 3% in the calculated shock wave velocity.

TABLE II. The stress ranges in which shock velocity data were available (Ref. 6).

Compound	Density ϵ (% TMD)	Lower stress limit (GPa)	Upper stress limit (GPa)
BeO	99.3	10	102
	92.4	9	93
	81.4	30	80
SiC	97.0	16	98
	94.2	42	88
	72.5	29	69
UO_2	94.0	24	161
	57.9	14	121

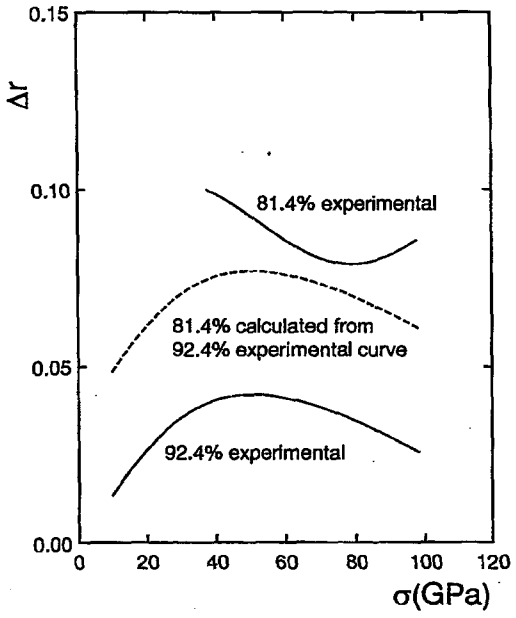

FIG. 4. Calculated deformation curves for 81.4% TMD BeO. The solid lines were calculated with Eq. (12) using data from Marsh (see Ref. 6). The dashed line was calculated with Eq. (16) from the Δr curve of 92.4% TMD BeO.

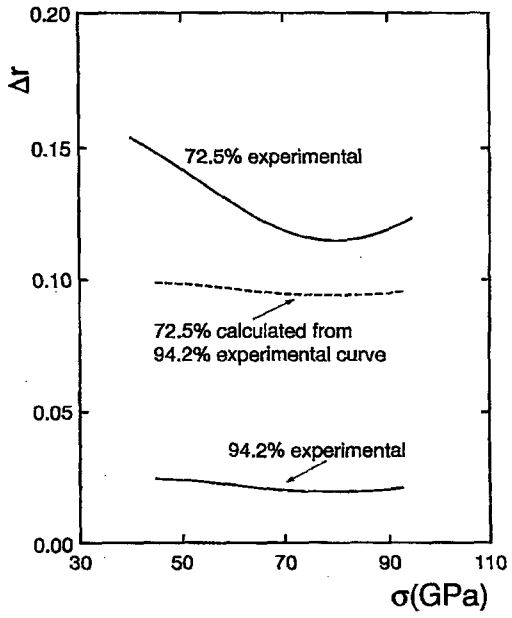

FIG. 5. Calculated deformation curves for 72.5% TMD SiC; the solid lines were calculated with Eq. (12) using data from Marsh (see Ref. 6). The dashed line was calculated with Eq. (16) from the Δr curve of 94.2% TMD SiC.

V. RELATION BETWEEN DEFORMATION CURVES

A. Introduction

The aim of the present model is to relate the shock wave velocities in two assemblies with different initial densities. Most of the available data consider precompacted assemblies.[6] It is, therefore, necessary to have a relation between the shock wave velocities in two precompacted assemblies. This relation can be derived from the relation between the Δr curves of a precompacted assembly and the Δr_0 curves of a loosely packed assembly found earlier.

B. Theory

The shock wave deformation Δr_i, in assembly i with a relative density of ϵ_i can be found from the total deformation Δr_0 and the initial deformation Δl_i,

$$\Delta r_i = \Delta r_0 - \Delta l_i. \tag{14}$$

The same applies for assembly j,

$$\Delta r_j = \Delta r_0 - \Delta l_j. \tag{15}$$

This means that

$$\Delta r_i = \Delta r_j + \Delta l_j - \Delta l_i. \tag{16}$$

C. Calculations

The Δr curve calculated with Eq. (16) for 81.4% TMD BeO from the 92.4% TMD BeO Δr curve is shown in Fig. 4. The 72.5% TMD SiC curve calculated from the 94.2% TMD SiC Δr curve is shown in Fig. 5. For the calculation of Δl, Eq. (7) was used with a loose packing density[10] of $\epsilon_0 = 50\%$ TMD.

To see if the Δr curves are material dependent, the Δr curve for a 72.5% TMD assembly was calculated from all BeO, SiC, and UO_2 curves. In Fig. 6 these Δr curves, calculated from 92.4% TMD BeO, 81.4% TMD BeO, and 57.9% TMD UO_2 data are shown compared to the curve of the 72.5% TMD SiC assembly.

D. Discussion

In Figs. 4 and 5 the predicted deformation curves for BeO and SiC are shown. In both calculations the calculated curves are lower than the curves to be predicted. The largest difference (33%) is found for SiC (see Fig. 5).

The Δr curves do not change shape when they are adapted in the present model to a different density with Eq. (16). This is due to the fact that the present model is a first-order approximation.

All three ceramics seem to have curves that are mutually exchangeable. The fact that the best predictions are made with the deformation curve of 57.9% TMD UO_2 and 81.4% TMD BeO indicates that the curves for BeO, SiC, and UO_2 are very similar.

The best predictions are made with the data of assemblies with densities closest to the density of the predicted curve. This is to be expected, because according to the model the Δr curves are an assembly property, and all assemblies are made of ceramics. Solid material properties are no longer incorporated in the Δr curves; thus, the error in the approximation should depend mainly on the relative density ϵ.

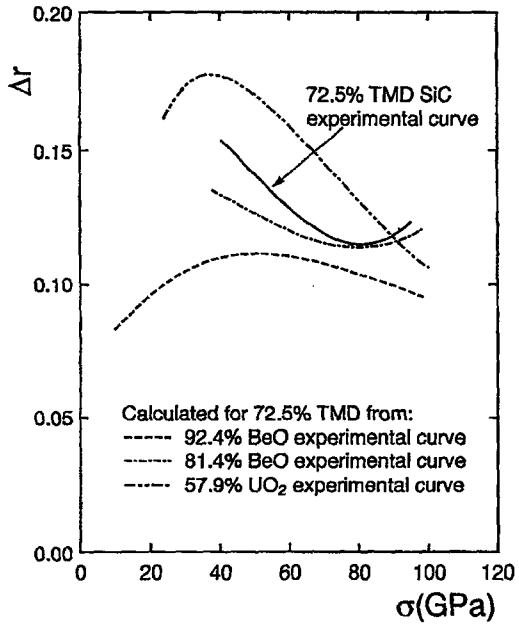

FIG. 6. Calculated deformation curves for 72.5% TMD using Δr curves from different densities compared to the experimental Δr curve of 72.5% TMD SiC. The experimental curves were calculated with experimental data from Marsh (see Ref. 6).

If a loose packing density of $\epsilon_0=50\%$ TMD is assumed, the initial deformation for a 72.5% dense assembly, calculated with Eq. (7), is $\Delta l=0.12$. If the maximum shock wave deformation ($\Delta r=0.18$ in Fig. 6 from 57.9% TMD UO_2) is added, the total deformation is $\Delta r_{0,\max}=0.30$.

The final contact area A after passage of the shock wave front can be calculated from

$$A=\pi R^2(2-\Delta r_0)\Delta r_0. \tag{17}$$

Thus, the maximum total deformation in Fig. 6, $\Delta r_{0,\max}=0.30$, corresponds with a final contact area, on transmission of the stable shock pressure of 51% of the maximum sphere cross section ($=\pi R^2$).

VI. SHOCK WAVE VELOCITY FROM DEFORMATION CURVE

A. Theory

With the relation between the deformation curves shock wave velocity data of one assembly can be used to predict the shock wave velocity in assemblies with other initial densities. The relation between the shock wave deformation Δr_i, and the shock wave velocity $U_{s,i}$ in assembly i can be found from Eq. (12),

$$\frac{1}{U_{s,i}}=\frac{1}{U_{s,\text{solid}}}+\frac{(\Delta r_i)}{(1-\Delta l_i)}\frac{1}{2u_{p,\text{solid}}}, \tag{18}$$

in which $\Delta r_i=\Delta r_0-\Delta l_i$. Substitution of Eq. (16) in Eq. (18) gives

$$\frac{1}{U_{s,i}}=\frac{1}{U_{s,\text{solid}}}+\frac{(\Delta r_j+\Delta l_j-\Delta l_i)}{(1-\Delta l_i)}\frac{1}{2u_{p,\text{solid}}}. \tag{19}$$

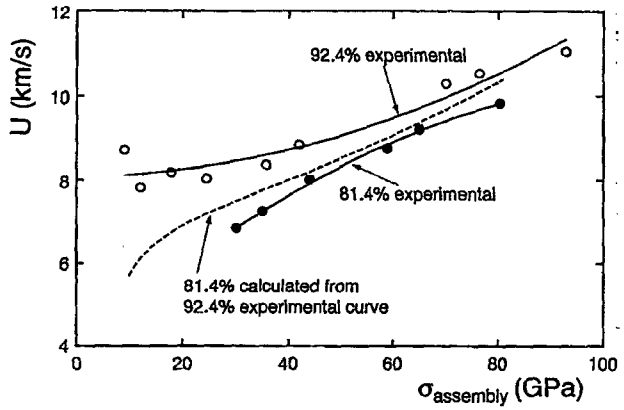

FIG. 7. The shock wave velocity U calculated for a 81.4% dense BeO assembly using the Δr curve from a 92.4% dense BeO assembly. Data are from Marsh (see Ref. 6).

The shock wave velocity $U_{s,i}$ in a porous assembly with density ϵ_i, therefore, can be predicted with the deformation curve of a porous assembly of density ϵ_j. The fact that the results in earlier calculations indicate that the deformation curves are not very sensitive to the type of ceramic suggests that the results for an assembly i of ceramic A could be used for calculations on assembly j of the ceramic B.

B. Calculations

For BeO and SiC assemblies there were two sets of data for different densities, which makes comparison possible. The $U_{s,i}$ curve calculated with Eq. (19) for 81.4% TMD BeO from the 92.4% TMD BeO Δr curve is shown in Fig. 7. The $U_{s,i}$ curve for 72.5% TMD SiC calculated from the 94.2% TMD SiC Δr curve is shown in Fig. 8. In Figs. 7 and 8 the calculations are compared with the experimental data from Marsh[6] and with the original shock wave data from which the Δr curves were calculated.

There was only one set of shock wave velocity data available[6] for a porous UO_2 assembly with a starting density

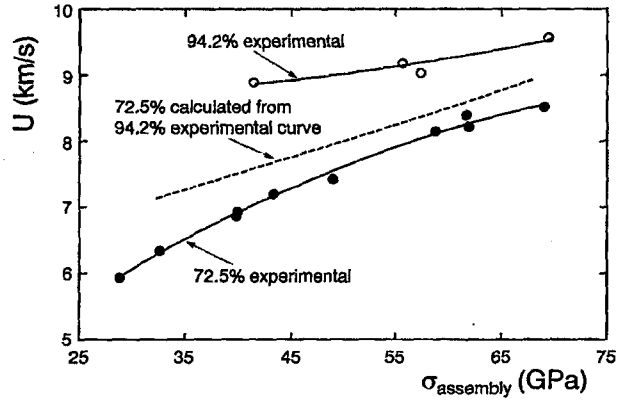

FIG. 8. The shock wave velocity U calculated for a 72.5% dense SiC assembly using the Δr curve from a 94.2% dense SiC assembly. Data are from Marsh (see Ref. 6).

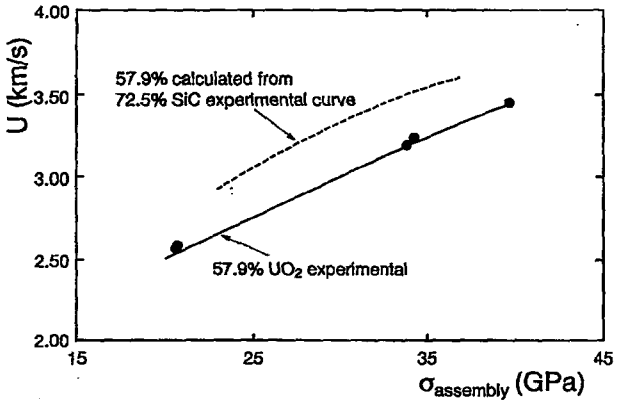

FIG. 9. The shock wave velocity U calculated for a 57.9% dense UO_2 assembly using the Δr curve from a 72.5% dense SiC assembly. Data are from Marsh (see Ref. 6).

above 50% TMD, apart from the 94.0% TMD data that were used to derive the "solid" Hugoniot. This prevented comparison with another UO_2 assembly. However, because the Δr curves seem to be material independent the Δr curve of 72.5% TMD SiC was used to calculate the $U_{s,i}$ curve for 57.9% TMD UO_2, with Eq. (19). The result is shown in Fig. 9.

To further study the effect of the material independence of the Δr curves on the calculation of $U_{s,i}$ curves the $U_{s,i}$ curve for 72.5% TMD SiC was calculated from the 81.4% TMD BeO Δr curve and the 57.9% TMD UO_2 Δr curve. The result is shown in Fig. 10.

C. Discussion

In Figs. 7 and 8 the predicted shock wave velocity curves for 81.4% TMD BeO and 72.5% TMD SiC are shown. These curves are predicted using the calculated Δr curves shown in Figs. 4 and 5. Within the range of available data the prediction of $U_{s,\text{assembly}}$ is always within 9% for BeO and SiC, when compared to data from Marsh.[6]

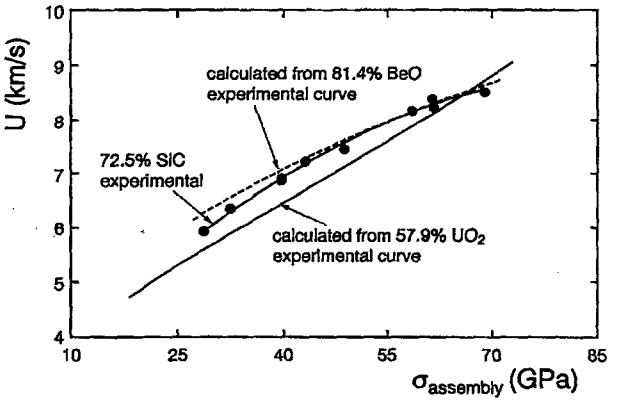

FIG. 10. The shock wave velocity U calculated for a 72.5% dense SiC assembly using the Δr curve from a 57.9% dense UO_2 assembly and the Δr curve from a 81.4% dense BeO assembly. Data are from Marsh (see Ref. 6).

The average deviation from the experimental curves is 3.9% for BeO and 5.7% for SiC. The calculation of the shock wave velocity curve for 57.9% TMD UO_2 with the 72.5% TMD SiC data, shown in Fig. 9, shows a maximum error of 9%. The calculation of the shock wave velocity in 72.5% TMD SiC with the deformation curve of 81.4% TMD BeO and 57.9% TMD UO_2 shown in Fig. 10 gives an even better result than the calculation in Fig. 8.

The results of the calculations shown in Figs. 9 and 10 indicate the possibility of a $\Delta r(\sigma,\epsilon)$ curve that would be applicable to all porous ceramic assemblies with ϵ>50% TMD.

In the model it was assumed that the deformation of the particles due to sintering or prepressing has the same effect on the contact area between the particles as the shock wave deformation. This is unlikely, because even with different static compaction techniques there is a difference in pore structure. Pressing, e.g., results in a different pore shape than sintering. In sintering the neck forming results in a different contact area than occurs after pressing.

It is therefore reasonable to assume that the initial contact area and its deformation depend on the pretreatments (such as pressing or sintering) applied to the material, before the shock wave is applied. This makes it hard to develop a general relation between the shock wave and initial deformation. The simple approximation presently used is applicable to all pretreatments.

The present model might be refined by a calculation of the initial deformation dependent on the pretreatment of the assembly. This refinement, however, would soon involve complex descriptions of porous assemblies and was, therefore, omitted for reasons of simplicity in the present model. Furthermore, this effect may not be to critical.

The particle size is likely to have an effect on the mechanisms, viz., fracture or plastic deformation at a given stress. If, however, plastic deformation is the most important mechanism the particle size probably has little effect. It is, therefore, assumed that the particle size has more effect on the energy dissipation effects in a shock wave than on the equilibrium properties.

Another simplification in the model was the principle of a head-on collision of two spheres. In an assembly the particle will not collide head on in general. In our current model, however, we only consider the longitudinal velocities. The contribution of particle contacts under small angles to the longitudinal velocity apparently outweighs other contributions. The model might be further developed to contain an average contact angle which could be calculated from contact forces in a porous assembly.[11]

VII. CONCLUSIONS

The presented deformation model is successful in the calculation of shock wave velocities in several assemblies of BeO, SiC, and UO_2. The model can be used to predict the shock wave velocity as a function of the shock stress for a porous assembly at several densities, when solid material properties and the data for one density are known. Even a very simple approximation of the internal shock stress in the

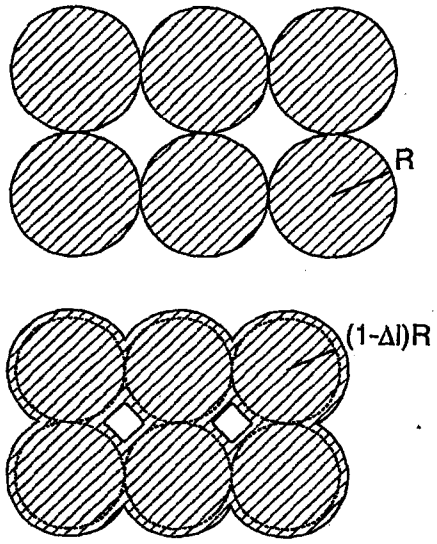

FIG. 11. Schematic representation of the isotropic compaction of a loosely packed assembly. The inscribed spheres shown in the compacted assembly have the same relative density as the original loose packing. The radius of the inscribed spheres is $(1-\Delta l)R$.

solid of the porous assembly gives an excellent correlation. The predictions are valid for densities above random loose packing density, which is about 50% TMD.

The success of the predictions indicates that the simplified presentation of a very complicated process used gives a good approximation. The resultant shock wave in a porous substance or powder seems to be transmitted only after a certain deformation of the particles is reached. This requires a novel approach to shock waves in porous substances as compared to solids.

The results furthermore seem to indicate that the deformation curves are not dependent on the solid material. This means that there might be a generally applicable deformation curve for, e.g., ceramics, as calculated in this article.

ACKNOWLEDGMENTS

The authors wish to thank Professor B. Scarlett from the Delft University of Technology, N. W. A. Broug, geotechnical consulting engineer, and E. G. de Jong of the Prins Maurits Laboratory for discussions. This work was performed under the auspices of the IOP Technical Ceramic programme under Contract No. 89.A027

APPENDIX: ISOTROPIC COMPACTION OF AN ARRAY OF SPHERES

If an array of spheres is isotropically compacted the density of the assembly after compaction can be related to the deformation of the spheres.

In Fig. 11 an array of spheres is shown before and after compaction. The spheres do not rearrange but are deformed over a length $R\Delta l$. Because there is no rearrangement of the spheres the relative density of the inscribed spheres (with a radius of $1-\Delta l$ times the original radius) is the same as the relative density of the spheres in the original array. This fact can be used to find an equation for the deformation Δl as a function of the relative density ϵ.

The total volume V_0 of a loosely packed assembly of N spheres, with radius R, can be found from

$$V_0=\frac{4\pi NR^3}{3\epsilon_0}, \tag{A1}$$

in which ϵ_0 is the relative density of the loosely packed assembly compared to the solid material density.

If the assembly with volume V is isotropically compressed and the spheres are deformed over a length of $R\Delta l$, we find for the volume V of the compressed assembly

$$V=\frac{4\pi NR^3(1-\Delta l)^3}{3\epsilon_0}. \tag{A2}$$

The relative density of the compressed assembly ϵ can be found from the total solid volume after compaction, which must be equal to the volume of the spheres in the original array, to obey mass conservation, and the new total volume V. This yields

$$\epsilon=\frac{\frac{4}{3}\pi NR^3}{V}. \tag{A3}$$

Combination of Eqs. (A3) and (A2) gives an expression for Δl as a function of the relative densities,

$$\Delta l=1-\left(\frac{\epsilon_0}{\epsilon}\right)^{1/3}. \tag{A4}$$

The density of a random loose packing of irregular particles varies between 45% TMD and 55% TMD. In the following Δl is calculated with $\epsilon_0=50\%$ TMD. The maximum error of $\pm 10\%$ in the relative density leads to a maximum error of $\pm 3.3\%$ in the initial deformation.

With a relative density for the loosely packed assembly of $\epsilon_0=50\%$ TMD and a maximum density of $\epsilon_i=100\%$ TMD, the maximum value for Δl $(\epsilon_0=50\%, \epsilon_i=100\%)=0.21$. This maximum value does not apply to the sphere deformation in a shock wave. Because the deformation in the shock wave is not isotropic it is possible to find values for the shock wave deformation $\Delta r_0>0.21$.

[1] K. Oh and P. Persson, J. Appl. Phys. **66**, 4736 (1989).
[2] G. A. Simons and H. H. Legner, J. Appl. Phys. **53**, 943 (1982).
[3] D. J. Rasky and M. R. McHenry, in *Shock Compression of Condensed Matter—1989*, edited by S. C. Schmidt, J. N. Johnson, and L. W. Devison (Elsevier, New York, 1990), pp. 101–104.
[4] J. E. Flinn, R. L. Williamson, R. A. Berry, R. N. Wright, Y. M. Gupta, and M. Williams, J. Appl. Phys. **64**, 1446 (1988).
[5] J. Gao, B. Shao, and K. Zhang, J. Appl. Phys. **69**, 7547 (1991).
[6] *LASL Shock Hugoniot Data*, edited by S. P. Marsh (University of California Press, Berkeley, 1980).
[7] C. L. Hoenig and C. S. Yust, Ceram. Bull. **60**, 1175 (1981).
[8] P. Boogerd and A. C. Van der Steen, in *Shock Waves and High-Strain-Rate Phenomena in Materials—1990*, edited by M. A. Meyers, L. E. Murr, and K. P. Staudhammer (Dekker, New York, 1992), p. 443.
[9] T. Taniguchi, K. Kondo, and A. Sawaoka, in *Shock Waves in Condensed Matter*, edited by Y. M. Gupta (Plenum, New York, 1986), p. 773.
[10] R. M. German, *Particle Packing Characteristics* (Metal Powder Industries Federation, Princeton, NJ, 1989), p. 176.
[11] N. W. A. Broug, Technology Today (Czechoslovak Academy of Sciences and Conneco) **3**, 153 (1991).